Neurobiology of Pain 12 (2022) 100109

Contents lists available at ScienceDirect

Neurobiology of Pain

journal homepage: www.sciencedirect.com/journal/neurobiology-of-pain

Cell specific regulation of NaV1.7 activity and trafficking in rat nodose ganglia neurons

Santiago I. Loya-López [a,b,1], Paz Duran [a,b,1], Dongzhi Ran [c], Aida Calderon-Rivera [a,b], Kimberly Gomez [a,b], Aubin Moutal [d], Rajesh Khanna [a,b,*]

[a] Department of Molecular Pathobiology, College of Dentistry, New York University, New York, USA
[b] NYU Pain Research Center, 433 First Avenue, New York, NY 10010, USA
[c] Department of Pharmacology, College of Medicine, The University of Arizona, Tucson, AZ 85724, USA
[d] School of Medicine, Department of Pharmacology and Physiology, Saint Louis University, Saint Louis, MO 63104, USA

ARTICLE INFO

Keywords:
NaV1.7
Trafficking
CRMP2
Numb
Nodose ganglia neurons

ABSTRACT

The voltage-gated sodium NaV1.7 channel sets the threshold for electrogenesis. Mutations in the gene encoding human NaV1.7 (*SCN9A*) cause painful neuropathies or pain insensitivity. In dorsal root ganglion (DRG) neurons, activity and trafficking of NaV1.7 are regulated by the auxiliary collapsin response mediator protein 2 (CRMP2). Specifically, preventing addition of a small ubiquitin-like modifier (SUMO), by the E2 SUMO-conjugating enzyme Ubc9, at lysine-374 (K374) of CRMP2 reduces NaV1.7 channel trafficking and activity. We previously identified a small molecule, designated **194**, that prevented CRMP2 SUMOylation by Ubc9 to reduce NaV1.7 surface expression and currents, leading to a reduction in spinal nociceptive transmission, and culminating in normalization of mechanical allodynia in models of neuropathic pain. In this study, we investigated whether NaV1.7 control via CRMP2-SUMOylation is conserved in nodose ganglion (NG) neurons. This study was motivated by our desire to develop **194** as a safe, non-opioid substitute for persistent pain, which led us to wonder how **194** would impact NaV1.7 in NG neurons, which are responsible for driving the cough reflex. We found functioning NaV1.7 channels in NG neurons; however, they were resistant to downregulation via either CRMP2 knockdown or pharmacological inhibition of CRMP2 SUMOylation by **194.** CRMP2 SUMOylation and interaction with NaV1.7 was consered in NG neurons but the endocytic machinery was deficient in the endocytic adaptor protein Numb. Overexpression of Numb rescued CRMP2-dependent regulation on NaV1.7, rendering NG neurons sensitive to **194.** Altogether, these data point at the existence of cell-specific mechanisms regulating NaV1.7 trafficking.

Introduction

Voltage-gated sodium channels (VGSCs) are key players in the initiation and propagation of action potentials in excitable cells (Waxman & Zamponi, 2014). To date, nine pore-forming alpha subunits of VGSCs – NaV1.1 to NaV1.9 (Catterall et al., 2005) – have been identified, each with distinct voltage-dependent properties with NaV1.7, NaV1.8 and NaV1.9 playing important roles in electrogenesis in sensory neurons (Bennett et al., 2019). During action potential generation, NaV1.7 contributes to the rising phase and amplifies subthreshold stimuli (Waxman & Zamponi, 2014; Bennett et al., 2019; Meents et al., 2019). NaV1.7 is preferentially expressed in peripheral sensory neurons, including dorsal root ganglion (DRG), nodose ganglion (NG), sympathetic ganglion (Kwong et al., 2008) and trigeminal ganglion (Liu et al., 2019). For over two decades now, NaV1.7 channels have been a focus of intense research as a validated target for pain. Mutations in the gene *SCN9A* coding for NaV1.7, lead to the both gain- or loss-of-function phenotypes in humans, manifesting a severe neuropathic pain or an insensitivity to pain, respectively (Dib-Hajj et al., 2010). Additionally, dysregulation in NaV1.7 expression has been reported to contribute to the development of chronic pain (Laedermann et al., 2013; Zhang & Dougherty, 2014). Genetic deletion of NaV1.7 in mice or

* Corresponding author at: Department of Molecular Pathobiology, College of Dentistry, New York University, 433 1st Avenue, 433 First Avenue, Room 720, New York, NY 10010, USA.
E-mail address: rk4272@nyu.edu (R. Khanna).
[1] Contributed equally.

https://doi.org/10.1016/j.ynpai.2022.100109
Received 20 October 2022; Received in revised form 10 November 2022; Accepted 10 November 2022
Available online 12 November 2022

pharmacological antagonism with NaV1.7-specific blockers leads to led to reduced pain-like behaviors (Shields et al., 2018), thus highlighting the importance of NaV1.7 in nociception.

The properties and function of NaV1.7 channels are subject to regulation in sensory neurons (Chew & Khanna, 2018; Chew et al., 2019). In DRG neurons, we reported that the membrane expression and activity of NaV1.7 channels is regulated by an auxiliary cytosolic protein, the collapsin response mediator protein 2 (CRMP2) (Dustrude et al., 2013; Dustrude et al., 2016). We further demonstrated that CRMP2 physically interacts with NaV1.7 channels and its modification by addition of a small ubiquitin-like modifier (SUMO) at lysine-374 (K374), in a process called SUMOylation, promotes surface expression and activity of NaV1.7 (Dustrude et al., 2013; Dustrude et al., 2016). In another study, we reported that excitability of DRG neurons is correlated with an increased SUMOylation of CRMP2, likely accounted for by increased expression and activity of NaV1.7 in animal models of neuropathic pain (Moutal et al., 2020). To interrogate the in vivo function of CRMP2 SUMOylation, we created CRMP2 SUMO-null knock-in ($CRMP2^{K374A/K374A}$) mice in which Lys374 was changed to Ala (Moutal et al., 2020). In sensory neurons of these mice, NaV1.7 membrane location and function were reduced compared to wildtype mice. Behavioral evaluation of $CRMP2^{K374A/K374A}$ mice revealed a reduction in unpleasant thermal sensitivity but no alterations in depressed or repetitive, compulsive-like behaviors while inflammatory, acute, or visceral pain in $CRMP2^{K374A/K374A}$ mice was indifferent from their wildtype littermates did not alter their behavior (Moutal et al., 2020). Notably, $CRMP2^{K374A/K374A}$ mice were refractory to development of mechanical allodynia in a chronic neuropathic pain model (Moutal et al., 2020).

Building on the mechanism of indirect regulation of NaV1.7 by SUMOylated CRMP2, we next set out to harness it to develop a small molecule for control of chronic pain. Screening of a compound library identified a small molecule, designated **194**, that prevented CRMP2 SUMOylation by the E2 SUMO-conjugating enzyme Ubc9 to uncouple the CRMP2-Ubc9 interaction which led to reduced NaV1.7 surface expression and currents, a reduction in spinal nociceptive transmission, and culminated in normalization of mechanical allodynia in models of neuropathic pain (Cai et al., 2021).

In delving deeper into determining how NaV1.7 activity was reduced upon CRMP2 deSUMOylation, we discovered that it relied on endocytosis (Dustrude et al., 2016; Cai et al., 2021; Gomez et al., 2021). Specifically, the reduction in NaV1.7 activity imposed by CRMP2 deSUMOylation was prevented by blocking clathrin-mediated endocytosis with Pitstop2 or by deleting the endocytic adaptor protein Numb (Dustrude et al., 2016); the neuronal precursor cell expressed developmentally downregulated-4 type 2 (Nedd4-2), which is recruited by Numb to mark NaV1.7 for endocytosis by monoubiquitination (Laedermann et al., 2013); or the epidermal growth factor receptor pathway substrate 15 (Eps15), which binds, in turn, to a monoubiquitinated NaV1.7 to allow clathrin vesicles to form (Woelk et al., 2006; Horvath et al., 2007; Dustrude et al., 2013; Gomez et al., 2021). Inhibiting clathrin assembly, with Piststop2 –a clathrin-mediated endocytosis inhibitor, in nerve-injured $CRMP2^{K374A/K374A}$ mice precipitated mechanical allodynia in mice otherwise resistant to developing persistent pain (Gomez et al., 2021). Together, these studies identify a signaling program utilizing CRMP2 SUMOylation to control the trafficking and activity of NaV1.7 channels, establishing a novel mechanism for the development and potential treatment of chronic pain.

Several studies have described NaV1.7 functions in non-nociceptive sensory processes, including olfaction (Ahn et al., 2011; Weiss et al., 2011), acid sensing (Smith et al., 2011), and the cough reflex (Muroi et al., 2011). With respect to the latter, the cough reflex is controlled by the sensory neurons within the nodose ganglion of mammals (Kwong et al., 2008), which innervate a broad spectrum of receptors in cardiovascular, gastrointestinal and respiratory organs. Their central axons transmit information regarding heart rate, blood pressure, bronchial irritation and gastrointestinal distension to the central nervous system and terminate in the nucleus of the solitary tract of the medulla (Zhuo et al., 1997). NaV1.7 channels have been shown to be functionally expressed in guinea pig nodose ganglion (Muroi et al., 2011). Here, they contribute to NG excitability as inferred from experiments wherein viral infection with short hairpin RNA (shRNA) against NaV1.7 reduced action potential firing (Muroi et al., 2013). It was further demonstrated that pharmacological blockade of NaV1.7 channels with Protoxin III and Huwentoxin IV, decreased the number of citric acid-evoked physiological as well as ovalbumin-sensitized cough responses in guinea pigs (Kocmalova et al., 2021).

Here, we asked if regulation of NaV1.7 by CRMP2-SUMOylation is conserved in NG neurons. Our impetus for this arose from our interest in developing **194** as a safe, non-opioid alternative for chronic pain, prompting us to ask if **194** would affect NaV1.7 in NG neurons. Though we observed functional NaV1.7 channels in NG neurons, they were unaffected by CRMP2 knockdown or by pharmacological antagonism of CRMP2 SUMOylation by **194**. Overexpression of Numb, levels of which were reduced compared to DRG neurons, recapitulated CRMP2-dependent regulation on NaV1.7 such that now NG neurons were sensitive to **194**. Altogether, these data point to cell-specific regulation of NaV1.7.

Methods

Ethics approval

The Institutional Animal Care and Use Committee (IACUC) of New York University approved all experiments (Protocol 202100104). All procedures were conducted in accordance with the *Guide for the Care and Use of Laboratory Animals* published by the National Institutes of Health.

Materials

All chemicals, unless noted, were purchased from Sigma (St Louis, MO). **194** (benzoylated 2-(4-piperidinyl)-1,3-benzimidazole analog; molecular weight 567.6) was obtained from TCG Lifesciences (Kolkata, India) and $>$ 99 % purity was confirmed using HPLC and resuspended in DMSO for in vitro use (Cai et al., 2021).

Animals

Pathogen-free adult female Sprague-Dawley rats (150–200 g; Charles River Laboratories, Wilmington, MA) were housed in temperature-controlled (23 $\pm$ 3ºC) and light-controlled (12-h light/12-h dark cycle; lights on at 7:00–19:00) rooms. Standard rodent chow and water were available *ad libitum*. All efforts were made to minimize animal suffering.

Isolation and culture of rat nodose ganglion (NG) neurons

Female Sprague-Dawley rats were euthanized through an isoflurane overdose and decapitated. Nodose ganglion were identified and collected and then subsequently incubated in DMEM media containing neutral protease (3.125 mg mL^{-1}, cat. no. LS02104, Worthington, Lakewood, NJ) and collagenase type I (5 mg mL^{-1}, cat no. LS004194, Worthington, Lakewood, NJ). The ganglion were digested for approximately 40 min at 37 °C under gentle agitation Dissociated cells were collected by centrifugation for 5 min at 800 $\times$ g at 25 °C. The supernatant was discarded, and the pellet was resuspended in complete DMEM media containing 1 % penicillin/streptomycin sulfate (10,000 μL^{-1}, stock), 30 ng mL^{-1} of nerve growth factor and 10 % fetal bovine serum (Hyclone). Collected nodose ganglion neurons were then transfected with Numb plasmid (pCMV-FLAG-Numb) (Nishimura et al., 2003), Invitrogen Stealth RNAi™ siRNA Negative Control (scramble siRNA) (cat. no. 12935300, Thermo Fisher Scientific) or CRMP2 siRNA (5′ GTAAACTCCTTCCTCGTGT-3′; obtained from Thermo Fisher

Scientific) (Brittain et al., 2009b; Brittain et al., 2012; Dustrude et al., 2016) using the rat neuron Nucleofector™ solution (program O-003; Amaxa Biosystems, Lonza Cologne, Germany). The pmaxGFP™ Vector (program O-003; Amaxa Biosystems, Lonza Cologne, Germany) was transfected as a reporter gene. Cells were plated onto 12-mm poly-D-lysine/laminin-coated glass coverslips and maintained at 37 °C and 5 % CO_2 in complete DMEM media. Successfully transfected cells were identified by GFP fluorescence.

Isolation and culture of rat dorsal root ganglion (DRG) neurons

Female Sprague-Dawley rats (100 g) were euthanized according to institutionally approved procedures with an isoflurane overdose and decapitated. Skin, muscle and vertebrae were cut to expose lumbar and thoracic dorsal root ganglion (DRG) as previously described (Moutal et al., 2020). Briefly, nerve roots were trimmed and DRGs were carefully removed and placed in DMEM media and digested for 1 h at 37 °C under gentle agitation with 3.125 mg/mL protease and 5 mg/mL collagenase. Dissociated cells were collected by centrifugation for 5 min at 800g at 25 °C, resuspended in DMEM media containing 1 % penicillin/streptomycin sulfate (10,000 μL-1, stock), 30 ng mL-1 of nerve growth factor and 10 % fetal bovine serum (Hyclone) and plated on poly- D-lysine-coated 15 mm coverslips for proximity ligation assays.

Proximity ligation assay

The proximity ligation assay (PLA) was performed as described previously (Moutal et al., 2017; Moutal et al., 2018b; Moutal et al., 2020). To visualize protein–protein interactions by microscopy. This assay is based on paired complementary oligonucleotide-labelled secondary antibodies that can hybridize and amplify a red fluorescent signal only when bound to two corresponding primary antibodies whose targets are in close proximity (within 30 nm). Briefly, nodose ganglia neurons or dorsal root ganglia neurons (as a positive control) were fixed using ice-cold methanol for 5 min and allowed to dry at room temperature. The proximity ligation assay was performed according to the manufacturer's protocol using the Duolink Detection Kit with PLA PLUS and MINUS probes for mouse and rabbit antibodies (Duolink in situ detection reagents red, cat. no. DUO92008; Duolink in situ PLA probe anti-rabbit MINUS, cat. no. DUO92005; Duolink in situ PLA probe anti-mouse PLUS, cat. no. DUO92001, Sigma-Aldrich). Primary antibodies (1/1000 dilution) were incubated for 1 h at RT; NaV1.7 (cat. no. MABN41; Millipore, RRID:AB_10808664), CRMP2 (cat. no. C2993; Sigma-Aldrich, RRID:AB_1078573), SUMO1 (cat. no. S8070; Sigma-Aldrich, RRID:AB_477543) and CRMP2 (cat. no. 11096; Tecan, immunobiological lab, RRID:AB_494511). Cells were then stained with 49,6-diamidino-2-phenylindole (DAPI, 50 mg/mL) to detect cell nuclei and mounted in ProLong Diamond Antifade Mountant (cat. no. P36961, Life Technologies Corporation). Immunofluorescent micrographs were acquired using a Plan-Apochromat 63x/1.4 oil CS2 objective on a Leica SP8 confocal microscope operated by the LAS X microscope software (Leica). Camera gain and other relevant settings were kept constant throughout imaging sessions. Image J was used to count the number of PLA puncta per cell.

Patch-clamp electrophysiology

Whole-cell voltage-clamp and current-clamp recordings were performed between 18 h after culture or 48 h after transfection at room temperature using an EPC 10 HEKA amplifier. Electrodes were pulled from filamented borosilicate glass capillaries (Warner Instruments) with a P-97 electrode puller (Sutter Instruments) to final resistances of 2.5–3.5 MΩ when filled with internal solutions. Whole-cell capacitance and series resistance were compensated. Linear leak currents were digitally subtracted by P/4 method for voltage clamp experiments, and bridge balance was compensated in current clamp experiments. Signals were filtered at 10 kHz and digitized at 10–20 kHz. Cells in which series resistance or bridge balance was >15 MΩ or fluctuated by >30 % over the course of an experiment were omitted from datasets. Analysis was performed by using Fitmaster software.

In experiments where CRMP2 SUMOylation was prevented by the addition of 5 μM **194**, the compound was incubated in the tissue culture well overnight, ~14 h before the experiment. In experiments in which clathrin-mediated endocytosis was prevented with 20 μM Pitstop2 (cat. no. ab120687; Abcam), the compound was incubated in the tissue culture well for 30 min before the experiment.

For voltage-clamp sodium current recordings, the external solution contained 140 mM NaCl, 30 mM tetraethylammonium chloride, 10 mM D-glucose, 3 mM KCl, 1 mM $CaCl_2$, 0.5 mM $CdCl_2$, 1 mM $MgCl_2$, and 10 mM HEPES (pH 7.3 and 310–315 mOsm); and the internal solution consisted of: 140 mM CsF, 10 mM NaCl, 1.1 mM Cs-EGTA, and 15 mM HEPES (pH 7.3 and 290–310 mOsm).

Nodose ganglion neurons were subjected to current–voltage (I-V) and activation/inactivation voltage protocols as follows: a) For the I-V protocol, cells were held at a potential of −60 mV and depolarized by 150-millisecond voltage steps from −70 mV to +60 mV in +5-mV increments, the resulting currents were normalized to the cell size, expressed as cell capacitance in pF, to get the current density and the corresponding peak current density. The voltage-dependence activation of sodium channels was analyzed as a function of current vs voltage. b) Inactivation protocol: from a holding potential of −60 mV, cells were subjected to 1 s hyperpolarizing/repolarizing pulses between −120 to +10 mV (in + 10 mV steps) followed by a 200-millisecond test pulse to +10 mV. This incremental increase in membrane potential conditioned various proportions of sodium channels into a state of fast inactivation.

For whole cell current-clamp experiments, the external solution contained 154 mM NaCl, 5.6 mM KCl, 2 mM $CaCl_2$, 1 mM $MgCl_2$, 10 mM D-glucose and 8 mM HEPES (pH 7.4 and 310–315 mOsm); and the internal solution consisted of: 137 mM KCl, 10 mM NaCl, 1 mM $MgCl_2$, 1 mM EGTA, and 10 mM HEPES (pH 7.3 and 290–310 mOsm). Nodose ganglion neurons were held at their resting membrane potential and then subjected to a 100-millisecond depolarizing current step. The intensity of this current step was adjusted until the neurons fired an action potential to determine the rheobase of the cells. Additionally, depolarizing current injections of 0–120 pA were applied to nodose ganglion cells to collect data on relative excitability, analyzed by counting the number of evoked action potentials during a 300-millisecond current step.

For I−V curves, functions were fitted to data using a non-linear least-squares analysis. I−V curves were fitted using a double Boltzmann function:

$$f = a + g1/\left(1 + \exp\left(x - V_{1/2}1/k1\right)\right) + g2/\left(1 + \exp\left(-\left(x - V_{1/2}2/k2\right)\right)\right)$$

Where × is the prepulse potential, $V_{1/2}$ is the midpoint potential, and k is the corresponding slope factor for single Boltzmann functions. Double Boltzmann fits were used to describe the shape of the curves, not to imply the existence of separate channel populations. Numbers 1 and 2 simply indicate the first and second midpoints; a along with g are fitting parameters.

Activation curves were obtained from the I−V curves by dividing the peak current at each depolarizing step by the driving force according to the equation: $G = I/(V_{mem} - E_{rev})$, where I is the peak current, V_{mem} is the membrane potential, and E_{rev} is the reversal potential. The conductance (G) was normalized against the maximum conductance (G_{max}). Inactivation curves were obtained by dividing the peak current recorded at the test pulse by the maximum current (I_{max}). Activation and inactivation curves were fitted with the Boltzmann equation.

Immunoblot preparation and analysis

Nodose ganglion and dorsal root ganglion lysates from female

Sprague-Dawley rats were loaded on 4–20 % Novex gels (cat. no. XP04205BOX; Thermo Fisher Scientific) and electrophoresed. Proteins were transferred for 1 h at 100 V using TGS [25 mM Tris, pH 8.5, 192 mM glycine, 0.1 % (mass/vol) SDS], 20 % (vol/vol) methanol as transfer buffer to PVDF membranes (0.45 μm; cat. no. IPFL00010; Millipore), preactivated in pure methanol. After transfer, the membranes were blocked at room temperature for 1 h with TBST (50 mM Tris·HCl, pH 7.4, 150 mM NaCl, 0.1 % Tween 20) with 5 % (mass/vol) nonfat dry milk, and then incubated separately in previously validated primary antibodies (1/1000 dilution): NaV1.7 (cat. no. ab85015; Abcam, Resource Identification Portal (RRID):AB_2184346), βIII-Tubulin (cat. no. G7121; Promega, RRID:AB_430874), CRMP2 (cat. no. C2993; Sigma-Aldrich, RRID:AB_1078573), Numb (cat. no. ab4147; Abcam, RRID: AB_304320), Eps15 (cat. no. ab174291; Abcam, RRID:AB_2620176), Nedd4-2 (cat. no. ab131167, Abcam, RRID:AB_11157800), in TBST, 5 % (mass/vol) BSA, overnight at 4 °C. Following incubation in HRP-conjugated secondary antibodies (1/20000 dilution) from Jackson ImmunoResearch, blots were revealed by enhanced luminescence (WBKLS0500; Millipore) before exposure to photographic film.

Data analysis

Graphing and statistical analysis was performed with GraphPad Prism (Version 9). All data sets were checked for normality using the D'Agostino – Pearson test. Details of statistical tests, significance, and sample sizes are reported in the appropriate figure legends and tables. All data plotted represent mean ± SEM. The statistical significance of differences between means was calculated by performing Student *t*-test, nonparametric Mann Whitney test, nonparametric Kruskal-Wallis test or parametric analysis of variance (ANOVA) with a post hoc comparisons test (Dunn's multiple comparisons tests and Tukey's multiple comparisons test, respectively). Differences were considered significant if $p \leq 0.05$.

Results

NaV1.7 channels are functionally expressed in rat nodose ganglion (NG) neurons

252920186691400NaV1.7 channels in DRG neurons regulate nociceptive stimuli (Laedermann et al., 2013; Zhang & Dougherty, 2014). In addition to their expression in somatosensory neurons, NaV1.7 channels are also expressed in cell bodies of the nodose ganglion (NG) neurons. NaV1.7 in these vagal afferents project to the nucleus of the solitary tract or area postrema in the brainstem and are involved in the cough reflex (Zhang & Dougherty, 2014). To elucidate the role of NaV1.7 in rat nodose ganglion, we first evaluated their protein expression in this tissue. Immunoblotting with a validated antibody detected a band

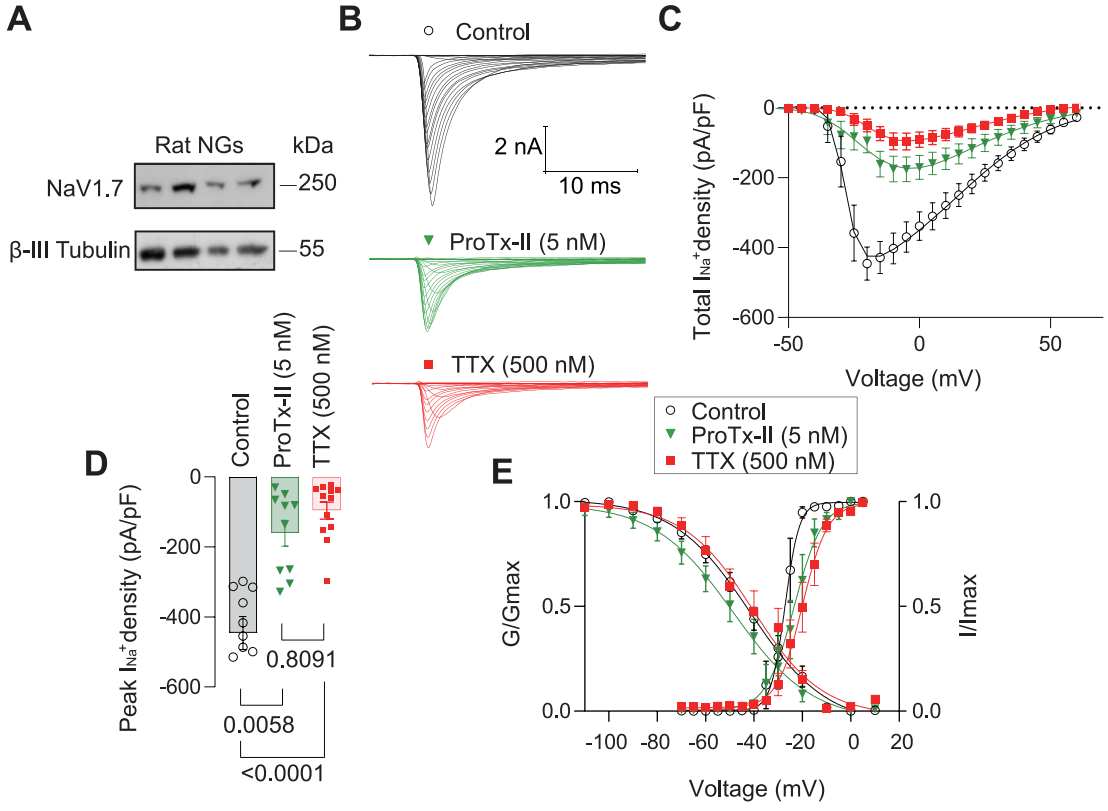

Fig. 1. Biochemical and electrophysiological characterization of NaV1.7 channels in rat nodose ganglion **(NG) neurons. A.** Western blot showing the expression of NaV1.7 channels in female rat NGs (n = 4). β-III tubulin was used as a loading control. **B.** Representative traces of Na^+ currents from rat nodose NGs in the presence of 0.1 % water (control; black open circles), 5 nM protoxin-II (ProTx-II; green triangles) or 500 nM tetrodotoxin (TTX; red squares) in external recording solution. **C.** Summary of sodium current density versus voltage relationship. In some control recordings, we observed a space clamp issue due to the very large (>6nA) sodium currents which resulted in a steep activation curve. **D.** Bar graphs of peak Na^+ current density, normalized to cell size (pA/pF) for sodium currents as indicated. Sodium current density was significantly smaller in NGs treated with 5 nM ProTx-II and 500 nM TTX ($p = 0.0058$ and $p < 0.0001$, respectively, Kruskal-Wallis test, followed by a Dunn's multiple comparisons test, $n = 10$–12 cells per condition), compared to the control group. Error bars indicate mean ± SEM. **E.** Boltzmann fits for normalized conductance (*G/Gmax*) voltage relationship for voltage dependent activation and inactivation of rat NGNs treated as indicated. Significant differences were observed in the gating properties of the ProTx-II group: $V_{0.5}$ and *k* values of activation ($p = 0.004$, $p = 0.0089$, respectively, one-way ANOVA, followed by a Tukey's multiple comparisons test, $n = 10$ cells per condition) and $V_{0.5}$ of inactivation ($p = 0.0450$, one-way ANOVA, followed by a Tukey's multiple comparisons test, $n = 10$ cells per condition). For full statistical analyses, see **Table S1**. Error bars indicate mean ± SEM. $V_{0.5}$ and *k* values for activation and inactivation are presented in Table 1. (For interpretation of the references to colour in this figure legend, the reader is referred to the web version of this article.)

corresponding to NaV1.7 in four independent rat nodose ganglia (Fig. 1**A**).

To assess if this translated into functional NaV1.7 channels, we carried out whole-cell voltage clamp experiments in dissociated rat NG neurons, in the absence or presence of tetrodotoxin (TTX) or the NaV1.7 selective blocker protoxin-II (ProTx-II, 5 nM) (Schmalhofer et al., 2008). Fig. 1**B** shows representative whole-cell currents. Sodium currents from cells held at a potential of − 60 mV and depolarized by 150-ms voltage steps from − 70 mV to + 60 mV in 5-mV increments were normalized to cell size to obtain current–voltage relationships (Fig. 1**C**). When cells were voltage clamped, large transient inward currents followed by smaller outward currents were seen in response to depolarizing steps. Mean peak current density (at −20 mV) was −445.8 ± 47.2 pA/pF (n = 9) (Fig. 1**D**). Five hundred nanomolar TTX reduced Na^+ currents by ~ 78 % (-96.4 ± 24.1 pA/pF; n = 12) compared to the control condition. The addition of 5 nM ProTx-II to the external recording solution resulted in an ~ 64 % decrease in NaV1.7 current density (-160.9 ± 36.88 pA/pF; n = 10) (Fig. 1**D**). The voltage dependence of activation was examined using a series of depolarizing test pulses from −60 mV. In the presence of ProTx-II, the channels activated at 5–9 mV more positive than channels in the control condition (Fig. 1**E and** Table 1). The midpoint of activation (estimated by fitting the data with a Boltzmann function) was significantly more positive for currents from ProTx-II treated NG neurons (-20.4 ± 1.9 mV; n = 10) than currents from control condition (-28.2 ± 0.5 mV; n = 10). The midpoint of voltage dependence of steady-state fast inactivation of ProTx-II treated NG neurons was −48.6 ± 2.6 mV (n = 10), which was more negative than that from cells treated with water −41.7 ± 1.7 mV (n = 10) but the difference did not reach significance (Fig. 1**E and** Table 1). Collectively, these data show that the majority of sodium currents in rat NGs is via TTX-S NaV1.7 channels.

NaV1.7 channels contribute to excitability of nodose ganglion (NG) neurons

To test the involvement of NaV1.7 channels in the excitability of NG neurons, we next performed whole-cell current clamp experiments. We used a protocol where the number of evoked action potentials at increasing current injection steps (0–90 pA) and the current step at which the first action potential was elicited (rheobase) were measured in the absence or presence of 5 nM ProTx-II. Addition of ProTx-II decreased NG neuron excitability with a reduction in the number of elicited action potentials (Fig. 2**A, B and Table S1**) and a commensurate increase in rheobase (Fig. 2**C and Table S1**). These results demonstrate that NaV1.7 channels contribute to NG excitability.

CRMP2 is expressed in rat nodose ganglion neurons but does not regulate the function of NaV1.7 channels

In a series of studies, our group previously reported that the activity and membrane expression of NaV1.7 channels in DRG neurons is regulated by their interaction with CRMP2 (Dustrude et al., 2013; Dustrude et al., 2016). When prevented from being SUMOylated, CRMP2 recruits an endocytic complex that promotes clathrin-mediated internalization of NaV1.7 channels, down-regulating their activity and ameliorating pain in acute and chronic models of pain (Dustrude et al., 2013; Dustrude et al., 2016; Moutal et al., 2020). Since our data shows that NaV1.7 channels represent the main TTX-S component in rat NGs and affect their excitability, we hypothesized that deletion of CRMP2 in NG would affect NaV1.7 channel function. We first confirmed that CRMP2 is expressed NG using a validated antibody against CRMP2 (Fig. 3**A**). Next, we silenced expression of CRMP2 in NG neurons using a previously validated siRNA against CRMP2 (Brittain et al., 2009b; Brittain et al., 2012; Dustrude et al., 2016) and measured sodium currents by performing whole-cell voltage clamp electrophysiology. To our surprise, neither the current amplitude nor the peak current density of sodium channels was affected by CRMP2 knockdown (Fig. 3**B-D and Table S1**).

Table 1
Gating properties of voltage-gated sodium channels in rat nodose ganglion neurons.

Condition	Activation		Inactivation	
	$V_{0.5}$	k	$V_{0.5}$	k
Fig. 1E				
Control	−28.16 ± 0.548 (10)	2.66 ± 0.464 (10)	−41.68 ± 1.715 (10)	−15.78 ± 1.642 (10)
ProTx-II (5 nM)	−20.45 ± 1.86 (10) p = 0.0004 respect to control	7.55 ± 1.64 (10) p = 0.0089 respect to control	−48.63 ± 2.621 (10) p = 0.1204 respect to control	−16.26 ± 2.65 (10) p = 0.9885 respect to control
TTX (500 nM)	−18.99 ± 0.88 (12) p < 0.0001 respect to control p = 0.6602 respect to ProTx-II	5.77 ± 0.76 (12) p = 0.1306 respect to control p = 0.3803 respect to ProTx-II	−40.42 ± 2.46 (12) p = 0.9215 respect to control p = 0.0450 respect to ProTx-II	−14.29 ± 2.29 (12) p = 0.9215 respect to control p = 0.0450 respect to ProTx-II
Fig. 3E				
Scramble siRNA	−29.78 ± 0.425 (16)	2.97 ± 0.376 (16)	−51.75 ± 1.528 (16)	−13.43 ± 1.601 (16)
CRMP2 siRNA	−31.30 ± 0.69 (11) p = 0.0589	2.66 ± 0.596 (11) p = 0.6453	−51.27 ± 2.353 (11) p = 0.8580	−13.21 ± 2.449 (11) p = 0.9369
Fig. 4D				
0.1 % DMSO	−28.85 ± 0.531 (17)	3.97 ± 0.464 (17)	−51.71 ± 1.742 (17)	−15.99 ± 1.992 (17)
194 (5 μM)	−27.828 ± 0.67 (23) p = 0.2647	4.84 ± 0.589 (23) p = 0.2796	−51.313 ± 1.135 (23) p = 0.8402	−11.50 ± 1.119 (23) p = 0.0632
Fig. 6D				
GFP + 0.1 % DMSO	−21.68 ± 0.469 (17)	2.78 ± 0.401 (17)	−45.71 ± 1.862 (17)	−14.17 ± 2.008 (17)
GFP + 194 (5 μM)	−22.65 ± 0.736 (12) p = 0.6778	3.78 ± 0.608 (12) p = 0.5386	−47.22 ± 1.081 (12) p = 0.9753	−9.48 ± 1.007 (12) p = 0.2385
GFP + 194 (5 μM) + Pitstop 2 (20 μM)	−19.95 ± 0.638 (12) p = 0.1644	4.16 ± 0.574 (12) p = 0.2354	−40.68 ± 1.722 (12) p = 0.2435	−13.73 ± 2.081 (12) p = 0.9537
Numb + DMSO	−22.14 ± 0.496 (20) p = 0.9595	4.33 ± 0.496 (20) p = 0.0743	−45.92 ± 1.986 (20) p = 0.9999	−14.95 ± 2.194 (20) p = 0.9947
Numb + 194 (5 μM)	−23.03 ± 0.481 (15) p = 0.3108	3.41 ± 0.388 (15) p = 0.8427	−48.91 ± 1.552 (15) p = 0.6067	−11.94 ± 1.551 (15) p = 0.7569
Numb + 194 (5 μM) + Pitstop 2 (20 μM)	−21.05 ± 0.705 (14) p = 0.9080	4.19 ± 0.562 (14) p = 0.1845	−41.91 ± 2.160 (14) p = 0.4634	−13.95 ± 2.198 (14) p = 0.9986

Values are means ± S.E.M. calculated from fits of the data from the indicated number (in parentheses) of cells to the Boltzmann equation. $V_{0.5}$, midpoint potential (mV) for voltage-dependent activation or inactivation; k, slope factor. Data were analyzed as follows: Fig. 1E, one-way ANOVA with Tukey's post hoc test; Fig. 3E and 4D, unpaired t-test; Fig. 6D, Dunnett's multiple comparisons test.

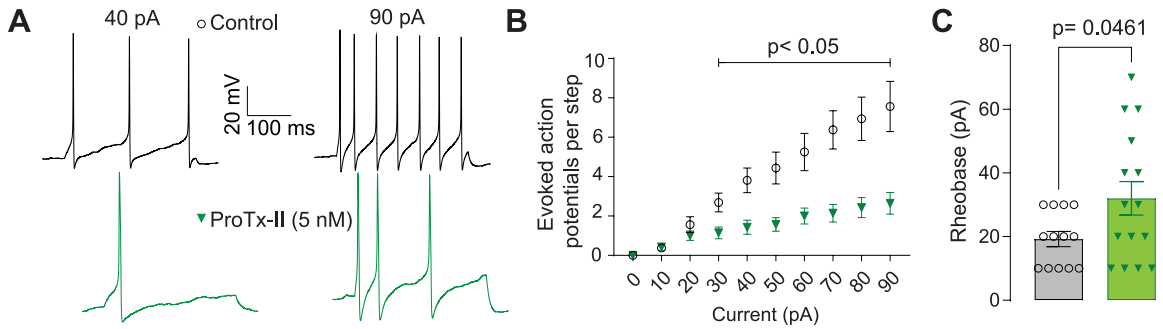

Fig. 2. NaV1.7 channels regulate excitability of rat nodose ganglion **neurons. A.** Representative traces evoked by steps to 40 and 90 pA in control (0.1 % water)- and ProTx-II (5 nM)-treated NG neurons. **B.** Summary of the current-evoked action potentials in response to current injections between 0 and 90 pA in the presence of 0.1 % water or 5 nM ProTx-II in the external recording solution. The number of evoked action potentials was significantly lower in the presence of 5 nM ProTx-II between the 30-pA to the 90-pA steps ($p < 0.05$, multiple unpaired *t* tests, $n = 13$ to 15 cells per condition). **C** Quantification of the rheobase in the presence of 0.1 % water or 5 nM ProTx-II. Rheobase was significantly increased in the presence of ProTx-II ($p = 0.0461$, unpaired *t* test, $n = 13$ to 15 cells per condition). Error bars indicate mean ± SEM. For full statistical analyses, see **Table S1**.

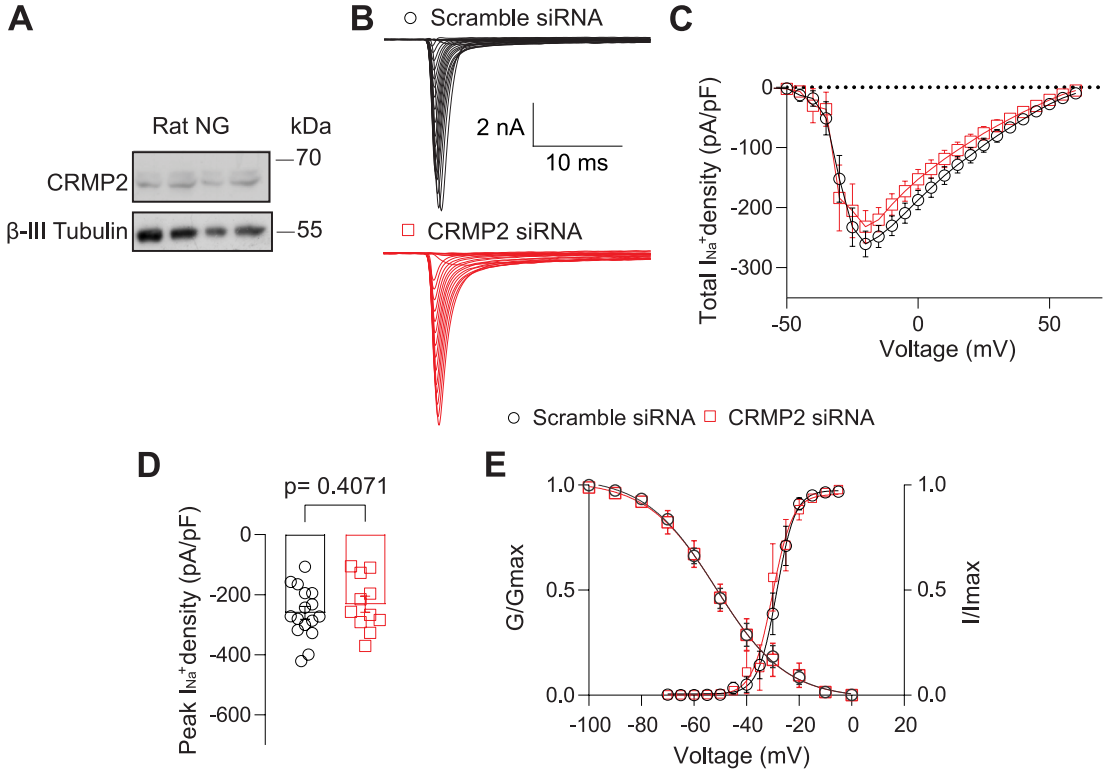

Fig. 3. CRMP2 silencing does not affect sodium currents in rat nodose ganglion neurons. A. Western blot showing expression of CRMP2 in rat NGs (n = 4). β -III tubulin was used as a loading control. **B.** Representative family of Na^+ current traces from rat nodose ganglion neurons transfected with Scramble siRNA (control; black open circles) or CRMP2 siRNA (red open squares) and recorded 48 h after transfection. **C.** Summary of sodium current density versus voltage relationship. **D.** Bar graphs of total peak Na^+ current density from NGs transfected with the indicated siRNAs. No difference was observed between groups (Unpaired *t* test, $n = 16$ to 11 cells per condition). **E.** Boltzmann fits of normalized conductance (*G/Gmax*) voltage relationship for voltage dependent activation and inactivation of rat NGs transfected as indicated. No difference was observed in the activation or inactivation properties of both groups (Unpaired *t* test, $n = 16$ to 11 cells per condition; See **Table S1** for detailed statistics). Error bars indicate mean ± SEM. (For interpretation of the references to colour in this figure legend, the reader is referred to the web version of this article.)

The voltage-dependent activation and inactivation properties of sodium channels were also unaffected upon CRMP2 deletion (Fig. 3**E and Table S1**). These findings suggest that CRMP2 does not regulate NaV1.7 function in NG neurons, supporting the possibility that NaV1.7 regulation may be different among different sensory cell types.

CRMP2 SUMOylation inhibitor 194 does not affect the activity of NaV1.7 channels

We have previously reported that genetic (Dustrude et al., 2016; Dustrude et al., 2017; Moutal et al., 2018a) or pharmacological inhibition (Cai et al., 2021; Braden et al., 2022; Li et al., 2022) of CRMP2 SUMOylation is sufficient to elicit a reduction in NaV1.7 activity and reverses pain-like behaviors. Here, we asked if the CRMP2 SUMOylation inhibitor **194** affects sodium currents in NG neurons. Overnight

incubation of cultured NGs with 5 μM **194** did not affect amplitude nor the peak current density of sodium channels (Fig. 4**A-C and Table S1**). The voltage-dependent activation and inactivation properties of sodium channels were also unchanged between control (0.1 % DMSO) and **194**-treated NG neurons (Fig. 4**D and Table S1**). Together with the data on deletion of CRMP2, these results support the notion that the mechanism of regulation of NaV1.7 by CRMP2 observed in DRGs is not present in NG neurons.

Reduced expression of the endocytic protein Numb in nodose ganglion

We reported that deSUMOylation of CRMP2 and ensuing loss of NaV1.7 membrane expression and activity in DRG neurons requires the association and recruitment of a complex of endocytic proteins comprising Nedd4-2, Numb, and Eps15 (Dustrude et al., 2016; Cai et al., 2021). If these endocytic proteins are absent, then NaV1.7 internalization does not occur, even in the presence of a deSUMOylated CRMP2 (Gomez et al., 2021). We first evaluated if CRMP2 is capable of being SUMOylated in NGs and can interact with NaV1.7 using the proximity ligation assay (PLA), a method that produces discrete fluorescent puncta when target proteins are within 40 nm of one another, thus revealing putative protein–protein interactions (Zhu et al., 2017). Dissociated cultures were plated for 1 day before performing PLA. We observed PLA puncta in DRG and NG using antibodies against SUMO1 and CRMP2 (Fig. 5**A**) and between NaV1.7 and CRMP2 (Fig. 5**B**). Similar levels of puncta were observed between DRG and NG for both protein interactions (Fig. 5**C, D**).

Another reason for the failure to recapitulate CRMP2 regulation of NaV1.7 in NG neurons may be due to the insufficient level of expression of these endocytic proteins, therefore, we analyzed the relative expression of Nedd4-2, Numb, and Eps15 in lysates of DRG and NG from female rats. Using previously validated antibodies (Gomez et al., 2021), we found that both DRG and NG expressed the three endocytic proteins (Fig. 6**A-D**). The level of expression of Nedd4-2 and Eps15 was unchanged between the ganglion (Fig. 6**B, D**). In contrast, Numb protein expression was relatively lower (by ~30 %) in NG compared to DRG (Fig. 6**C**). These results raise the intriguing hypothesis that the reduced Numb expression could underlie the inability of CRMP2 to regulate in NaV1.7 in NG neurons (Fig. 7).

Overexpression of the endocytic protein Numb restores CRMP2 regulation of NaV1.7

We previously published that reduction in NaV1.7 activity imposed by CRMP2 deSUMOylation was prevented by blocking clathrin-mediated endocytosis with Pitstop2 or by deleting the endocytic adaptor protein Numb (Dustrude et al., 2016). So, we performed additional experiments to test if incubation with the clathrin-mediated endocytosis Pitstop2 (20 μM, 30 min) would rescue pharmacological antagonism (by **194**) of NaV1.7 observed in Numb-overexpressing cells. Sodium currents in NG neurons transfected with GFP and incubated with **194** overnight and then with Pitstop2 for 30 min were no different from those without Pitstop2 (Fig. 7 **A-C and Tables S1**). In contrast, the decrease in sodium currents caused by 194 in NG neurons overexpressing Numb was reversed by Pitstop2 (Fig. 7 **A-C and Tables S1**). Voltage-dependent activation and inactivation properties were indistinguishable between any of the transfection and drug-treatment conditions (Fig. 7**D**, Table 1). These findings demonstrate that restoration of the endocytic machinery with Numb recapitulates **194**′s inhibition of NaV1.7, implicating CRMP2 deSUMOylation in control of NaV1.7, in a clathrin-dependent manner.

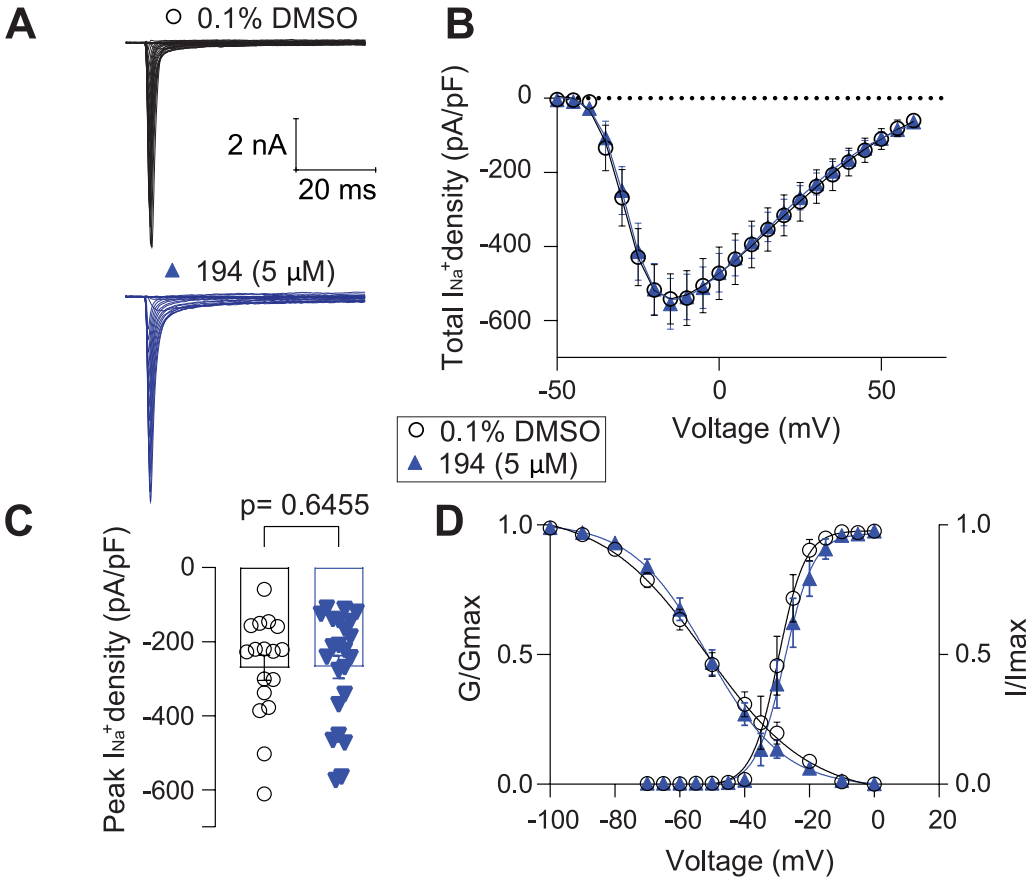

Fig. 4. The CRMP2 SUMOylation inhibitor 194 does not inhibit sodium currents in dissociated rat nodose ganglion neurons. A. Representative traces of Na^+ currents from rat nodose ganglion neurons incubated overnight with 0.1 % DMSO (control; black open circles) or 5 μM **194** (blue triangles). **B.** Summary of total sodium current density versus voltage relationship. **C.** Bar graphs of total peak Na^+ current density from NGs treated as indicated. No difference was observed between the groups (Unpaired *t* test, $n = 17$ to 23 cells per condition). **D.** Boltzmann fits of normalized conductance (*G/Gmax*) voltage relationship for voltage dependent activation and inactivation of rat NGs treated as indicated. No difference was observed in the activation or inactivation properties of both groups (Unpaired *t* test, $n = 17$ to 23 cells per condition). Error bars indicate mean ± SEM. $V_{0.5}$ and *k* values for activation and inactivation are presented in Table 1. (For interpretation of the references to colour in this figure legend, the reader is referred to the web version of this article.)

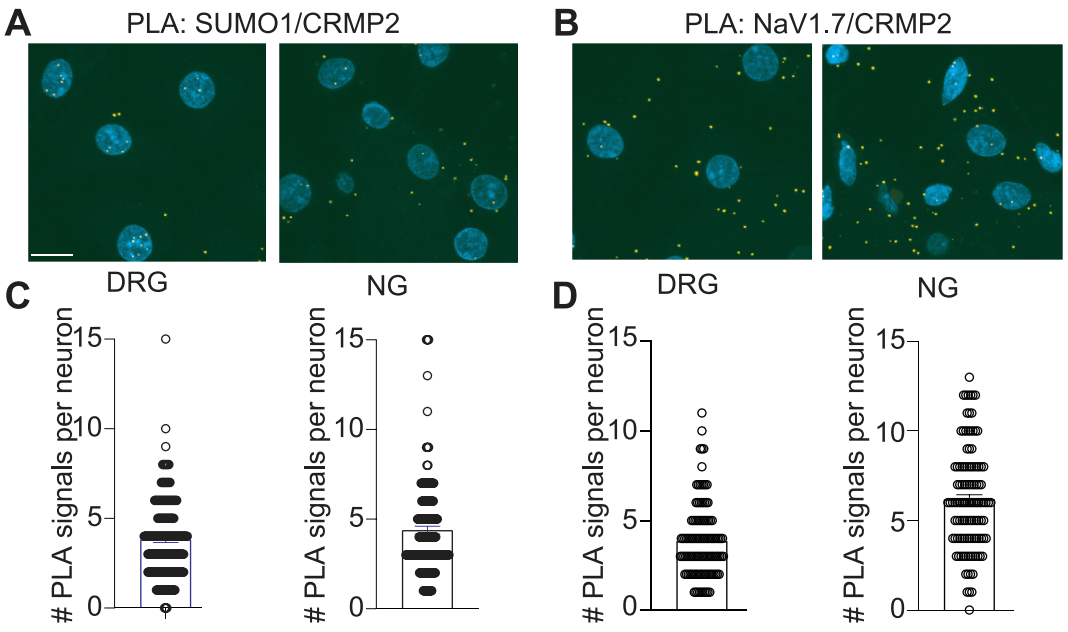

Fig. 5. CRMP2 is SUMOylated and binds to NaV1.7 in both dorsal root ganglion and nodose ganglion neurons. A. Pseudocolor representative images of rat DRG or NG cultures subjected to proximity ligation assay (PLA) between CRMP2 and SUMO1 (**A**) or between NaV1.7 and CRMP2 (**B**). The PLA immunofluorescence labeled sites of interaction between CRMP2 and SUMO1 or between NaV1.7 and CRMP2 (yellow puncta). Nuclei are labeled with the nuclear labeling dye 49,6-diamidino-2-phenylindole (DAPI). Scale bar: 10 μm. **C, D.** Quantification of PLA puncta per neuron (n = 93 to 165). (For interpretation of the references to colour in this figure legend, the reader is referred to the web version of this article.)

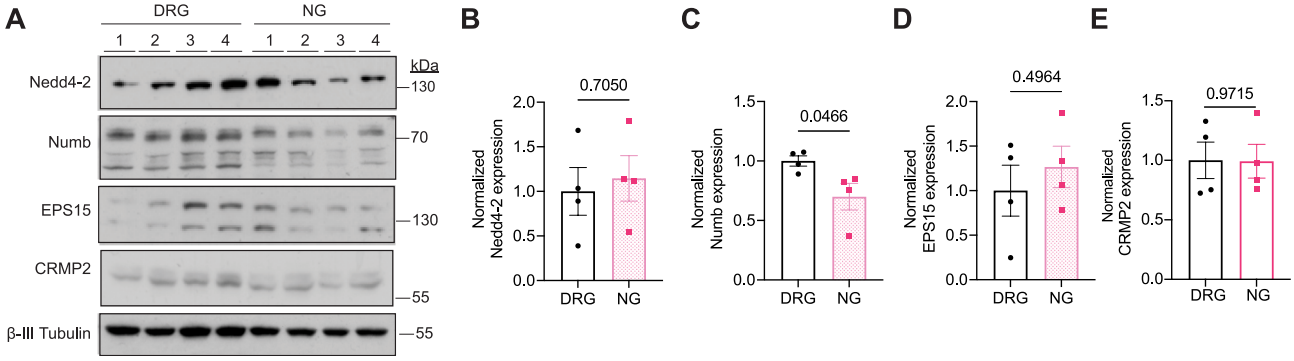

Fig. 6. Differential expression of endocytosis-related proteins in rat dorsal root ganglion (DRG) and nodose ganglion (NG). A. Representative immunoblots and summary of mean relative expression of Nedd4-2 (**B**), Numb (**C**) and Eps15 (**D**) in lysates of DRG and NG from four rats. β -III tubulin was used as a loading control. The means were compared with a two-tailed unpaired *t*-test with values as indicated. Only the expression of Numb protein was significantly reduced. Error bars indicate mean ± SEM.

Discussion

Here we report that neither genetic deletion of CRMP2 nor pharmacological antagonism of CRMP2 SUMOylation affects NaV1.7 channels in nodose ganglion (NG) neurons, revealing a cell-specific NaV1.7 regulatory mechanism. We also found that expression of the clathrin-mediated endocytic protein Numb is sufficient to restore inhibition of NaV1.7 by the CRMP2 SUMOylation inhibitor **194**.

We found that NaV1.7 accounts for ~ 64 % of the total tetrodotoxin-sensitive sodium currents in rat nodose ganglion neurons. Blockade of NaV1.7 with ProTx-II decreased action potential discharge and increased the minimum current needed to evoke an action potential, thus contributing to a reduced excitability of NG neurons. These findings are congruent with data from guinea pig NG neurons wherein NaV1.7 was reported to comprise ~65 % of the total sodium current (Muroi et al., 2011). In the same study, the authors also demonstrated that a short hairpin RNA against NaV1.7 inhibited the fast TTX-sensitive component of the sodium current by >60 % as well as reduced NG excitability. NaV1.7 accounts for a majority of the TTX-sensitive current in small diameter DRG neurons (Black et al., 2012). We have previously demonstrated that the activity and trafficking of NaV1.7 is under the control of CRMP2 in sensory neurons (Dustrude et al., 2013; Dustrude et al., 2016). CRMP2 associates with NaV1.7 and regulates its transport to the plasma membrane (Dustrude et al., 2013; Dustrude et al., 2016). Since most sodium current in NG neurons is via NaV1.7 channels, in the present work, we sought to investigate whether loss of CRMP2 expression could modify the current density of sodium channels. Surprisingly, when compared to our previous data in DRG neurons (Dustrude et al., 2013; Dustrude et al., 2016), we discovered that NaV1.7 channels in NG neurons are independent of CRMP2 regulation, as no changes were observed in sodium currents and their gating properties when CRMP2 was silenced. Binding between CRMP2 and NaV1.7 was also observed in NG neurons.

In studying regulation of NaV1.7 by CRMP2, we identified that loss of SUMOylation of CRMP2 results in decreased binding to NaV1.7, resulting in reduced membrane localization, current density, and

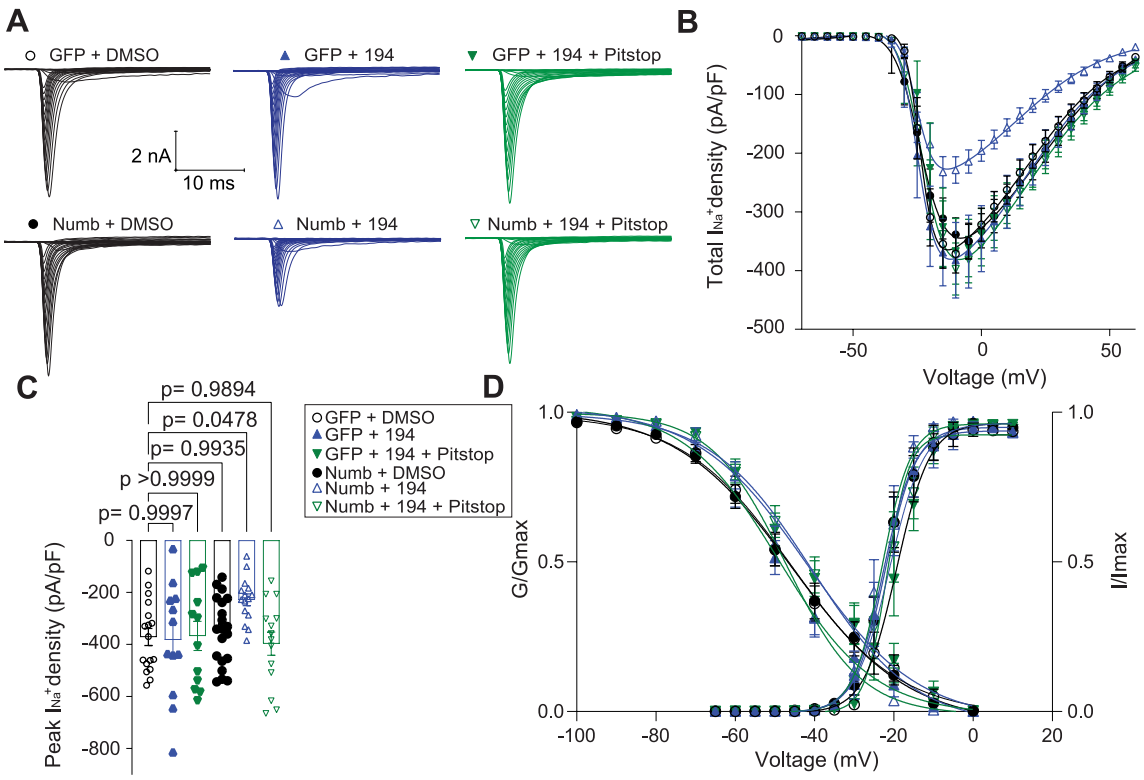

Fig. 7. Overexpression of Numb restores CRMP2 regulation of NaV1.7. A. Representative traces of Na^+ currents from rat nodose ganglion neurons incubated overnight with 0.1 % DMSO (control; black open circles) or 5 μM **194** (blue triangles) and in the absence or presence of the clathrin-inhibitor 20 μM Pitstop2 (incubated 30 min before the recordings). **B** Summary of total sodium current density versus voltage relationship. **C** Bar graphs of total peak Na^+ current density from NGs treated as indicated. The overexpression of Numb significantly decreased the amplitude and density of total sodium currents in the presence of 5 μM **194** (One-way ANOVA, followed by a Dunnett's test, $n = 12$ to 20 cells per condition). **D.** Boltzmann fits for normalized conductance (*G/Gmax*) voltage relationship for voltage dependent activation and inactivation of rat NGNs pre-treated as indicated. A significant difference was observed in the activation $V_{0.5}$ of the GFP + 194 + Pitstop 2 group (One-way ANOVA, followed by a Dunnett's test, $n = 12$ to 20 cells per condition). Error bars indicate mean ± SEM. (For interpretation of the references to colour in this figure legend, the reader is referred to the web version of this article.)

neuronal excitability (Dustrude et al., 2013; Dustrude et al., 2016). Blocking CRMP2 SUMOylation with a SUMO-impaired CRMP2-K374A mutant triggered NaV1.7 internalization in a clathrin-dependent manner involving the E3 ubiquitin ligase Nedd4-2 and endocytosis adaptor proteins Numb and Eps15 (Dustrude et al., 2016). A small fifteen amino acid inhibiting peptide encompassing the CRMP2-SUMOylation site phenocopied the genetic ablation of CRMP2 (François-Moutal et al., 2018). Finally, CRMP2 SUMO-null knock-in ($CRMP2^{K374A/K374A}$) mice in which Lys374 was changed to Ala also had reduced NaV1.7 membrane location and function compared to wildtype mice (Moutal et al., 2020). Leveraging these findings, we identified a small molecule (**1 9 4**) that inhibited CRMP2 SUMOylation by uncoupling the interaction between the E2-SUMO-cojugating enzyme Ubc9 and CRMP2 to reduce NaV1.7 trafficking and current density in DRG neurons from mice, rats, pigs, and humans (Cai et al., 2021). Compound **194** was antinociceptive across a range of acute and neuropathic pain models in male and female mice and rats (Braden et al., 2022; Li et al., 2022). A recent study demonstrated that BW-031, a selective NaV1.7 blocker, inhibits inflammatory pain and cough reflex in guinea pigs (Tochitsky et al., 2021), a process regulated by nodose ganglion. In contrast, here we found that overnight incubation of rat NG neurons with **194** (5 μM; which represents approximately fourfold the IC_{50} of inhibition of NaV1.7 currents (Cai et al., 2021)), did not affect NaV1.7 currents or their voltage-dependent properties. If membrane expression and activity of NaV1.7 do not rely on CRMP2, it follows then that changes in CRMP2's SUMOylation state would not be expected to affect these channels, as we found in this work. The reticence of **194** to affect NaV1.7 currents coupled with the absence of any effect on NaV1.7 following CRMP2 ablation provides converging lines of evidence of a novel, cell-specific regulation of NaV1.7.

Using two experimental approaches, we demonstrate that the lack of regulation of NaV1.7 channels by CRMP2 in NGs may be correlated to the level of expression of proteins involved in clathrin-mediated endocytosis. In particular, the endocytic adaptor protein Numb (Santolini et al., 2000), which is a binding partner of CRMP2 (Nishimura et al., 2003), was expressed at lower levels in NGs compared to DRGs. Dominant-negative CRMP2 mutants or knockdown of CRMP2 inhibited endocytosis of a Numb-interacting protein L1, a neuronal cell adhesion molecule (Nishimura et al., 2003). Numb also interacts with Eps15 and the α-adaptin subunit of the AP-2 adaptor complex, establishing a firm role for this protein in clathrin-dependent endocytosis at the plasma membrane (Salcini et al., 1997; Berdnik et al., 2002). Forced overexpression of Numb in NGs rescued the inhibition of NaV1.7 with **194**, thus demonstrating that availability of Numb is a limiting step for the trafficking complex to couple to CRMP2 and the subsequent internalization of NaV1.7 channels, which is accordance with our previous reports (Dustrude et al., 2016, Gomez et al., 2021) where a hierarchical model of interaction between deSUMOylated CRMP2 and the proteins responsible for the clathrin-mediated endocytosis identified Numb as an adaptor and initiator of this process. Another inference from our results on **194** inhibiting NaV1.7 in Numb-over-expressing NGs is that CRMP2 is capable of being SUMOylated in NG, which was also directly demonstrated using the proximity ligation assay. When Numb expression is rate-limiting, Numb's role may shift from an endocytic adaptor to CRMP2, thus driving CRMP2 to participate in actin dynamics, axon growth or trafficking of other ion channels (Arimura et al., 2000; Arimura et al., 2005; Tahimic et al., 2006; Brittain et al., 2009a; Hensley et al., 2010; Morinaka et al., 2011). Additional studies will be required

to test the latter scenario. Several alternatively spliced forms of Numb transcripts have been reported, which under pathophysiological conditions can shift the balance between trafficking and endocytosis, and in the case of Alzheimer's disease, contribute to AD pathogenesis (Kyriazis et al., 2008). Whether differential expression of Numb isoforms is observed in NGs and under conditions of pathology remains to be determined.

The results presented here support further research on **194** for the treatment of neuropathic pain (Cai et al., 2021; Braden et al., 2022; Li et al., 2022), but not as an anti-tussive drug because it had no effect on NG neurons and is therefore unlikely to affect action potentials in the vagal nerve. Clinical studies using NaV1.7 blockers in individuals with persistent chronic cough showed no antitussive benefit, whereas administration of lidocaine suppressed cough in 1 of 2 patients but was accompanied by side effects (Roe et al., 2019). Though NaV1.7 has been implicated in inhibiting cough (Kocmalova et al., 2017; Sun et al., 2017; Tochitsky et al., 2020), its role in cough may be more complex if one considers that conduction in airway C-fiber axons is mediated mainly by NaV1.7 channels while initiation of action potentials at peripheral terminals is mediated by tetrodotoxin-resistant NaV1.8 channels (jugular C-fibers) or by NaV1.7 channels (nodose C-fibers and A-delta fibers) (Al-Kandery et al., 2021; Brozmanova et al., 2022). NaV1.8, which is not regulated by CRMP2 (Cai et al., 2021), appears to be a more suitable target for cough suppression as it was demonstrated that the NaV1.8 blocker A-803467 decreases prostaglandin E2-enhanced citric acid-induced cough (Tochitsky et al., 2020) and inhalation of A-803467 reduces capsaicin-induced coughing by ~65 % in guinea pigs (Brozmanova et al., 2022). As **194** does not block NaV1.7 in NG neurons, it is therefore unlikely to compromise the protective cough reflex.

Opioids including codeine, are potent suppressors of the cough reflex at therapeutic doses for the treatment of pain (Mukhopadhyay & Katzenstein, 2007; Nicolakis et al., 2020). Consequently, asphyxiation through aspiration can be the cause of ~40 % of all opioid related death (Nicolakis et al., 2020). While the underlying mechanisms are different, NaV1.7 and NaV1.8 blockers in development for the treatment of pain carry this liability. Here, we demonstrated that our pre-clinical candidate **194** had no effect on the function of NaV1.7 in nodose ganglion neurons that regulate cough. In conclusion, the salient findings of our work are: (i) NaV1.7 can be regulated by different mechanisms in neuronal subpopulations, (ii) CRMP2 does not regulate the function of nodose ganglion and is safe to target pharmacologically, and (iii) pain relief can be achieved without impacting cough, a strategy likely superior to current inhibitors of NaV1.7 and NaV1.8 undergoing clinical trials.

Funding

Supported by National Institutes of Health awards (NINDS (NS098772 and NS120663 to RK)).

Declaration of data availability

This Declaration acknowledges that this paper adheres to the principles for transparent reporting and scientific rigor of preclinical research and that all data supporting the results are presented in the manuscript.

CRediT authorship contribution statement

Santiago I. Loya-López: Formal analysis, Investigation, Methodology. **Paz Duran:** Formal analysis, Investigation, Methodology. **Dongzhi Ran:** Formal analysis, Investigation. **Aida Calderon-Rivera:** Formal analysis, Investigation, Methodology. **Kimberly Gomez:** Formal analysis, Investigation, Methodology. **Aubin Moutal:** Conceptualization, Formal analysis, Investigation, Methodology, Writing – review & editing. **Rajesh Khanna:** Conceptualization, Writing – Original Draft, Writing- Editing, Supervision, Project administration, Funding Acquisition.

Declaration of Competing Interest

R. Khanna is the co-founder of Regulonix LLC, a company developing non-opioids drugs for chronic pain. In addition, R. Khanna has patents US10287334 (Non-narcotic CRMP2 peptides targeting sodium channels for chronic pain) and US10441586 (SUMOylation inhibitors and uses thereof) issued to Regulonix LLC.

The remaining authors declare that they have no known competing financial interests or personal relationships that could have appeared to influence the work reported in this paper.

Data availability

Data will be made available on request.

Appendix A. Supplementary data

Supplementary data to this article can be found online at https://doi.org/10.1016/j.ynpai.2022.100109.

References

Ahn, H.S., Black, J.A., Zhao, P., Tyrrell, L., Waxman, S.G., Dib-Hajj, S.D., 2011. Nav1.7 is the predominant sodium channel in rodent olfactory sensory neurons. Mol. Pain 7, 32.

Al-Kandery, A.-S.-A., Rao, M.S., El-Hashim, A.Z., 2021. Prostaglandin E2 sensitizes the cough reflex centrally via EP3 receptor-dependent activation of NaV 1.8 channels. Respir. Res. 22, 296.

Arimura, N., Inagaki, N., Chihara, K., Ménager, C., Nakamura, N., Amano, M., Iwamatsu, A., Goshima, Y., Kaibuchi, K., 2000. Phosphorylation of collapsin response mediator protein-2 by Rho-kinase. Evidence for two separate signaling pathways for growth cone collapse. J. Biol. Chem. 275 (31), 23973–23980.

Arimura, N., Ménager, Céline, Kawano, Y., Yoshimura, T., Kawabata, S., Hattori, A., Fukata, Y., Amano, M., Goshima, Y., Inagaki, M., Morone, N., Usukura, J., Kaibuchi, K., 2005. Phosphorylation by Rho kinase regulates CRMP-2 activity in growth cones. Mol. Cell. Biol. 25 (22), 9973–9984.

Bennett, D.L., Clark, A.J., Huang, J., Waxman, S.G., Dib-Hajj, S.D., 2019. The role of voltage-gated sodium channels in pain signaling. Physiol. Rev. 99 (2), 1079–1151.

Berdnik, D., Török, T., González-Gaitán, M., Knoblich, J.A., 2002. The endocytic protein & #x3b1;-Adaptin is required for numb-mediated asymmetric cell division in Drosophila. Dev. Cell 3, 221–231.

Black, J.A., Frézel, N., Dib-Hajj, S.D., Waxman, S.G., 2012. Expression of Nav1.7 in DRG neurons extends from peripheral terminals in the skin to central preterminal branches and terminals in the dorsal horn. Mol. Pain 8, 82.

Braden K, Stratton HJ, Salvemini D & Khanna R. (2022). Small molecule targeting NaV1.7 via inhibition of the CRMP2-Ubc9 interaction reduces and prevents pain chronification in a mouse model of oxaliplatin-induced neuropathic pain. *Neurobiol. Pain (Cambridge, Mass)* **11,** 100082-.

Brittain, M.K., Brustovetsky, T., Sheets, P.L., Brittain, J.M., Khanna, R., Cummins, T.R., Brustovetsky, N., 2012. Delayed calcium dysregulation in neurons requires both the NMDA receptor and the reverse Na+/Ca2+ exchanger. Neurobiol. Dis. 46 (1), 109–117.

Brittain, J.M., Piekarz, A.D., Wang, Y., Kondo, T., Cummins, T.R., Khanna, R., 2009. An atypical role for collapsin response mediator protein 2 (CRMP-2) in neurotransmitter release via interaction with presynaptic voltage-gated calcium channels. J. Biol. Chem. 284 (45), 31375–31390.

Brozmanova, M., Buday, T., Konarska, M., Plevkova, J., 2022. The effect of the voltage-gated sodium channel NaV1.7 blocker PF-05089771 on cough in the guinea pig. Respir. Physiol. Neurobiol. 299, 103856.

Cai, S., Moutal, A., Yu, J., Chew, L.A., Isensee, J., Chawla, R., Gomez, K., Luo, S., Zhou, Y., Chefdeville, A., Madura, C., Perez-Miller, S., Bellampalli, S.S., Dorame, A., Scott, D.D., FranÃ§ois-Moutal, L., Shan, Z., Woodward, T., Gokhale, V., Hohmann, A. G., Vanderah, T.W., Patek, M., Khanna, M., Hucho, T., Khanna, R., 2021. Selective targeting of NaV1.7 via inhibition of the CRMP2-Ubc9 interaction reduces pain in rodents. *Sci. Transl. Med.* 13, eabh1314.

Catterall, W.A., Goldin, A.L., Waxman, S.G., 2005. International Union of Pharmacology. XLVII. Nomenclature and structure-function relationships of voltage-gated sodium channels. Pharmacol. Rev. 57 (4), 397–409.

Chew, L.A., Khanna, R., 2018. CRMP2 and voltage-gated ion channels: potential roles in neuropathic pain. Neuronal Signaling 2, -.

Chew, L.A., Bellampalli, S.S., Dustrude, E.T., Khanna, R., 2019. Mining the Na_v1.7 interactome: opportunities for chronic pain therapeutics. Biochem. Pharmacol. 163, 9–20.

Dib-Hajj, S.D., Cummins, T.R., Black, J.A., Waxman, S.G., 2010. Sodium channels in normal and pathological pain. Annu. Rev. Neurosci. 33 (1), 325–347.

Dustrude, E.T., Wilson, S.M., Ju, W., Xiao, Y., Khanna, R., 2013. CRMP2 protein SUMOylation modulates NaV1.7 channel trafficking. J. Biol. Chem. 288 (34), 24316–24331.
Dustrude, E.T., Moutal, A., Yang, X., Wang, Y., Khanna, M., Khanna, R., 2016. Hierarchical CRMP2 posttranslational modifications control NaV1.7 function. Proc. Natl. Acad. Sci. USA 113, E8443–E8452.
Dustrude, E.T., Perez-Miller, S., François-Moutal, L., Moutal, A., Khanna, M., Khanna, R., 2017. A single structurally conserved SUMOylation site in CRMP2 controls NaV1.7 function. Channels (Austin, Tex) 11 (4), 316–328.
François-Moutal, L., Dustrude, E.T., Wang, Y., Brustovetsky, T., Dorame, A., Ju, W., Moutal, A., Perez-Miller, S., Brustovetsky, N., Gokhale, V., Khanna, M., Khanna, R., 2018. Inhibition of the Ubc9 E2 SUMO-conjugating enzyme-CRMP2 interaction decreases NaV1.7 currents and reverses experimental neuropathic pain. Pain 159 (10), 2115–2127.
Gomez, K., Ran, D., Madura, C.L., Moutal, A., Khanna, R., 2021. Non-SUMOylated CRMP2 decreases NaV1.7 currents via the endocytic proteins Numb, Nedd4-2 and Eps15. Mol. Brain 14, 20.
Hensley, K., Christov, A., Kamat, S., Zhang, X.C., Jackson, K.W., Snow, S., Post, J., 2010. Proteomic identification of binding partners for the brain metabolite lanthionine ketimine (LK) and documentation of LK effects on microglia and motoneuron cell cultures. J. Neurosci. 30 (8), 2979–2988.
Horvath, C.A.J., Vanden Broeck, D., Boulet, G.A.V., Bogers, J., De Wolf, M.J.S., 2007. Epsin: inducing membrane curvature. Int. J. Biochem. Cell Biol. 39 (10), 1765–1770.
Kocmalova, M., Kazimierova, I., Barborikova, J., Joskova, M., Franova, S., Sutovska, M., 2021. The changes in expression of NaV1.7 and NaV1.8 and the effects of the inhalation of their blockers in healthy and ovalbumin-sensitized Guinea pig airways. *Membranes (Basel)* 11.
Kocmalova, M., Kollarik, M., Canning, B.J., Ru, F., Adam Herbstsomer, R., Meeker, S., Fonquerna, S., Aparici, M., Miralpeix, M., Chi, X.X., Li, B., Wilenkin, B., McDermott, J., Nisenbaum, E., Krajewski, J.L., Undem, B.J., 2017. Control of neurotransmission by NaV1.7 in human, guinea pig, and mouse airway parasympathetic nerves. J. Pharmacol. Exp. Ther. 361, 172–180.
Kwong, K., Carr, M.J., Gibbard, A., Savage, T.J., Singh, K., Jing, J., Meeker, S., Undem, B. J., 2008. Voltage-gated sodium channels in nociceptive versus non-nociceptive nodose vagal sensory neurons innervating guinea pig lungs. J. Physiol. 586, 1321–1336.
Kyriazis, G.A., Wei, Z., Vandermey, M., Jo, D.-G., Xin, O., Mattson, M.P., Chan, S.L., 2008. Numb Endocytic Adapter Proteins Regulate the Transport and Processing of the Amyloid Precursor Protein in an Isoform-dependent Manner: IMPLICATIONS FOR ALZHEIMER DISEASE PATHOGENESIS*. J. Biol. Chem. 283 (37), 25492–25502.
Laedermann, C.J., Cachemaille, M., Kirschmann, G., Pertin, M., Gosselin, R.-D., Chang, I., Albesa, M., Towne, C., Schneider, B.L., Kellenberger, S., Abriel, H., Decosterd, I., 2013. Dysregulation of voltage-gated sodium channels by ubiquitin ligase NEDD4-2 in neuropathic pain. J. Clin. Invest. 123 (7), 3002–3013.
Li, J., Stratton, H.J., Lorca, S.A., Grace, P.M., Khanna, R., 2022. Small molecule targeting NaV1.7 via inhibition of the CRMP2-Ubc9 interaction reduces pain in chronic constriction injury (CCI) rats. Channels (Austin, Tex) 16 (1), 1–8.
Liu, M., Zhong, J., Xia, L., Dou, N., Li, S., 2019. The expression of voltage-gated sodium channels in trigeminal nerve following chronic constriction injury in rats. Int. J. Neurosci. 129 (10), 955–962.
Meents, J.E., Bressan, E., Sontag, S., Foerster, A., Hautvast, P., Rösseler, C., Hampl, M., Schüler, H., Goetzke, R., Le, T.K.C., Kleggetveit, I.P., Le Cann, K., Kerth, C., Rush, A. M., Rogers, M., Kohl, Z., Schmelz, M., Wagner, W., Jørum, E., Namer, B., Winner, B., Zenke, M., Lampert, A., 2019. The role of Nav1.7 in human nociceptors: insights from human induced pluripotent stem cell-derived sensory neurons of erythromelalgia patients. Pain 160 (6), 1327–1341.
Morinaka, A., Yamada, M., Itofusa, R., Funato, Y., Yoshimura, Y., Nakamura, F., Yoshimura, T., Kaibuchi, K., Goshima, Y., Hoshino, M., Kamiguchi, H., Miki, H., 2011. Thioredoxin mediates oxidation-dependent phosphorylation of CRMP2 and growth cone collapse. Sci. Signal 4, ra26.
Moutal, A., Wang, Y., Yang, X., Ji, Y., Luo, S., Dorame, A., Bellampalli, S.S., Chew, L.A., Cai, S., Dustrude, E.T., Keener, J.E., Marty, M.T., Vanderah, T.W., Khanna, R., 2017. Dissecting the role of the CRMP2-neurofibromin complex on pain behaviors. Pain 158 (11), 2203–2221.
Moutal, A., Dustrude, E.T., Largent-Milnes, T.M., Vanderah, T.W., Khanna, M., Khanna, R., 2018a. Blocking CRMP2 SUMOylation reverses neuropathic pain. Mol. Psychiatry 23 (11), 2119–2121.
Moutal, A., Li, W., Wang, Y., Ju, W., Luo, S., Cai, S., François-Moutal, L., Perez-Miller, S., Hu, J., Dustrude, E.T., Vanderah, T.W., Gokhale, V., Khanna, M., Khanna, R., 2018b. Homology-guided mutational analysis reveals the functional requirements for antinociceptive specificity of collapsin response mediator protein 2-derived peptides. Br. J. Pharmacol. 175 (12), 2244–2260.
Moutal, A., Cai, S., Yu, J., Stratton, H.J., Chefdeville, A., Gomez, K., Ran, D., Madura, C. L., Boinon, L., Soto, M., Zhou, Y., Shan, Z., Chew, L.A., Rodgers, K.E., Khanna, R., 2020. Studies on CRMP2 SUMOylation-deficient transgenic mice identify sex-specific Nav1.7 regulation in the pathogenesis of chronic neuropathic pain. Pain 161 (11), 2629–2651.
Mukhopadhyay, S., Katzenstein, A.L., 2007. Pulmonary disease due to aspiration of food and other particulate matter: a clinicopathologic study of 59 cases diagnosed on biopsy or resection specimens. Am. J. Surg. Pathol. 31, 752–759.
Muroi, Y., Ru, F., Kollarik, M., Canning, B.J., Hughes, S.A., Walsh, S., Sigg, M., Carr, M.J., Undem, B.J., 2011. Selective silencing of Na(V)1.7 decreases excitability and conduction in vagal sensory neurons. J. Physiol. 589, 5663–5676.
Muroi, Y., Ru, F., Chou, Y.L., Carr, M.J., Undem, B.J., Canning, B.J., 2013. Selective inhibition of vagal afferent nerve pathways regulating cough using Nav 1.7 shRNA silencing in guinea pig nodose ganglia. Am. J. Physiol. Regul. Integr. Comp. Physiol. 304, R1017–R1023.
Nicolakis, J., Gmeiner, G., Reiter, C., Seltenhammer, M.H., 2020. Aspiration in lethal drug abuse-a consequence of opioid intoxication. Int. J. Legal Med. 134 (6), 2121–2132.
Nishimura, T., Fukata, Y., Kato, K., Yamaguchi, T., Matsuura, Y., Kamiguchi, H., Kaibuchi, K., 2003. CRMP-2 regulates polarized Numb-mediated endocytosis for axon growth. Nat. Cell Biol. 5 (9), 819–826.
Roe, N.A., Lundy, F.T., Litherland, G.J., McGarvey, L.P.A., 2019. Therapeutic targets for the treatment of chronic cough. Curr. Otorhinolaryngol. Rep. 7 (2), 116–128.
Salcini, A.E., Confalonieri, S., Doria, M., Santolini, E., Tassi, E., Minenkova, O., Cesareni, G., Pelicci, P.G., Di Fiore, P.P., 1997. Binding specificity and in vivo targets of the EH domain, a novel protein–protein interaction module. *Genes Dev.* 11, 2239–2249.
Santolini, E., Puri, C., Salcini, A.E., Gagliani, M.C., Pelicci, P.G., Tacchetti, C., Di Fiore, P. P., 2000. Numb is an endocytic protein. *J. Cell Biol.* 151, 1345–1352.
Schmalhofer, W.A., Calhoun, J., Burrows, R., Bailey, T., Kohler, M.G., Weinglass, A.B., Kaczorowski, G.J., Garcia, M.L., Koltzenburg, M., Priest, B.T., 2008. ProTx-II, a selective inhibitor of NaV1.7 sodium channels, blocks action potential propagation in nociceptors. Mol. Pharmacol. 74 (5), 1476–1484.
Shields, S.D., Deng, L., Reese, R.M., Dourado, M., Tao, J., Foreman, O., Chang, J.H., Hackos, D.H., 2018. Insensitivity to pain upon adult-onset deletion of Nav1.7 or its blockade with selective inhibitors. J. Neurosci. 38 (47), 10180–10201.
Smith, E.S.J., Omerbašić, D., Lechner, S.G., Anirudhan, G., Lapatsina, L., Lewin, G.R., 2011. The molecular basis of acid insensitivity in the African naked mole-rat. Science 334 (6062), 1557–1560.
Sun, H., Kollarik, M., Undem, B.J., 2017. Blocking voltage-gated sodium channels as a strategy to suppress pathological cough. Pulm. Pharmacol. Ther. 47, 38–41.
Tahimic, C.G.T., Tomimatsu, N., Nishigaki, R., Fukuhara, A., Toda, T., Kaibuchi, K., Shiota, G., Oshimura, M., Kurimasa, A., 2006. Evidence for a role of Collapsin response mediator protein-2 in signaling pathways that regulate the proliferation of non-neuronal cells. Biochem. Biophys. Res. Commun. 340 (4), 1244–1250.
Tochitsky, I., Jo, S., Andrews, N., Kotoda, M., Doyle, B., Shim, J., Talbot, S., Roberson, D., Lee, J., Haste, L., Jordan, S.M., Levy, B.D., Bean, B.P., Woolf, C.J. (2020). Inhibiting cough by silencing large pore-expressing airway sensory neurons with a charged sodium channel blocker. *bioRxiv*, 2020.2012.2007.414763.
Tochitsky, I., Jo, S., Andrews, N., Kotoda, M., Doyle, B., Shim, J., Talbot, S., Roberson, D., Lee, J., Haste, L., Jordan, S.M., Levy, B.D., Bean, B.P., Woolf, C.J., 2021. Inhibition of inflammatory pain and cough by a novel charged sodium channel blocker. Br. J. Pharmacol. 178 (19), 3905–3923.
Waxman, S.G., Zamponi, G.W., 2014. Regulating excitability of peripheral afferents: emerging ion channel targets. Nat. Neurosci. 17 (2), 153–163.
Weiss, J., Pyrski, M., Jacobi, E., Bufe, B., Willnecker, V., Schick, B., Zizzari, P., Gossage, S.J., Greer, C.A., Leinders-Zufall, T., Woods, C.G., Wood, J.N., Zufall, F., 2011. Loss-of-function mutations in sodium channel Nav1.7 cause anosmia. Nature 472 (7342), 186–190.
Woelk, T., Oldrini, B., Maspero, E., Confalonieri, S., Cavallaro, E., Di Fiore, P.P., Polo, S., 2006. Molecular mechanisms of coupled monoubiquitination. Nat. Cell Biol. 8 (11), 1246–1254.
Zhang, H., Dougherty, P.M., 2014. Enhanced excitability of primary sensory neurons and altered gene expression of neuronal ion channels in dorsal root ganglion in paclitaxel-induced peripheral neuropathy. Anesthesiology 120, 1463–1475.
Zhu, X., Zelmer, A., Wellmann, S., 2017. Visualization of protein-protein interaction in nuclear and cytoplasmic fractions by co-immunoprecipitation and in situ proximity ligation assay. J. Vis. Exp.
Zhuo, H., Ichikawa, H., Helke, C.J., 1997. Neurochemistry of the nodose ganglion. Prog. Neurobiol. 52, 79–107.